

Flame Propagation and Burning Rates of Methane-Air in a Closed Combustion Vessel

Mohd Suardi Suhaimi, Aminuddin Saat* and Mazlan Abd Wahid

*Department of Thermofluids, Faculty of Mechanical Engineering,
Universiti Teknologi Malaysia, 81310 Skudai, Johor, Malaysia
E-mail: amins@mail.fkm.utm.my

ABSTRACT

The propagation and burning rates of methane-air mixtures were investigated at initial atmospheric pressure with temperature range of 298-302K and equivalence ratio range of 0.8 to 1.3. Experiments were performed in a cylindrical constant volume combustion chamber where the mixture is ignited by centrally located electrodes. The images of spherically expanding flame were observed and recorded using schlieren photography technique with high speed camera system. Analysis of the flame area yield flame radii and further burning rates in term of outwardly flame speed propagation can be calculated. Results shows that smooth spherical flames were observed throughout the flame propagation for all equivalence ratios. The fastest flame propagation was recorded at equivalence ratio 1.0 and 1.2. In addition, flame speed of each equivalence ratio exhibits small fluctuation probably arising from acoustic disturbance. This disturbance becomes more apparent at higher equivalence ratio.

Keywords:

Methane-air, flame speed, schlieren, constant volume

1. INTRODUCTION

The determination of combustion characteristics such as laminar burning velocity is of primary importance as it relevance to both laminar and turbulent premixed combustion. Detailed knowledge from accurate measurement of laminar premixed flames will provide valuable insight on propagation rates, heat release, flammability limits, quenching and emission characteristics. Another useful insight from laminar premixed flame is that it could serve as a preliminary data in understanding a much more complex combustion such as turbulent non-premixed combustion and also combustion process in practical combustor such as internal combustion

engine where the initial stage of combustion involves laminar premixed combustion.

Several methods have been used to determine this parameter such as flat flame [1,2], counterflow flame [3,4] and spherically expanding flame[5-8]. These experiments also enable the study of another parameter which is the stretch that acts on the flame front. This parameter is a combination of curvature and strain rate and is described by Markstein length [9]. For spherically expanding flame, the stretch can be obtained analytically from flame speed and radius. The unstretched flame speed on the other hand could be obtained from linear extrapolation of the flame speed and stretch curve [10]. However it is sensitive to the data obtained from experiment. Earlier work by Taylor [5] involved the differentiation of the spherically expanding flame radius to obtain flame speed, stretch, Markstein length and burning rate. Tahtouh et al [9] compared three different analysis methods namely the polynomial fitting, raw radius differentiation and a new method that involves resolution of Clavin's equation to determine the aforesaid parameters. They reported that each method yield different results.

The objective of this study is to determine the burning rates of methane-air mixture in term of flame speed propagation using images from schlieren photography. Methane is one of the abundant gaseous fuels in nature that also exist in nature as the flammable part of biogas [11]. Schlieren photography is a photography technique that makes use of the density gradient in the vicinity of the object of interest. This is particularly useful in combustion as it generates a region with defined density gradient arising from heat generated. Though the method is not novel, obtaining improved images could improve results from literature. Schlieren photography also permits the exclusion of experiments that produce cellular flame for the purpose of determining flame speed, Markstein length and burning rates

[11]. This exclusion is important as the occurrence of cellularity will render the smooth flame front assumption. Comparison with data from literature may also serve as a calibration to the rig setup used in this study.

2. EXPERIMENTAL SETUP

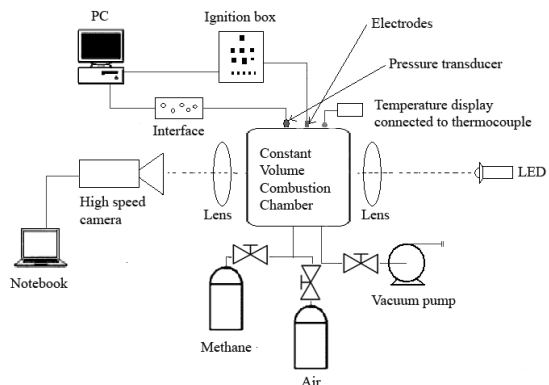


Figure 1. Experimental setup

Figure 1 shows a schematic of experimental setup consisting of a cylindrical constant volume combustion chamber with a volume of 29.3 litre and two 190mm quartz windows, ignition system, Phantom 7.1 high speed camera, collimating and decollimating lens and an LED light source. Ignition was initiated and controlled with Labview 7.1 software that also serves as a data logger recording pressure rise during combustion.

The cylindrical combustor used in his study is equipped a pair of opposing spark electrodes to provide ignition at the center of the combustor. After a vacuum was created in the combustion chamber by a vacuum pump, the chamber was filled with methane and dry air using partial pressure technique which correspond to the desired equivalence ratio. The initial pressure for each experiment was set at atmospheric pressure, while the initial temperature was in the range of 298 to 302K. Ignition was controlled using a desktop computer with LabView 7.1 software connected to the ignition box after the capacitor was charged. The 190 mm windows provide wide optical access and currently limited by the lens used. A pair of collimating and decollimating lens with 150 mm diameter was used. Both lenses have a focal length of 700 mm. The developing flame videos were recorded at 2000 frames per second. A 1.5W LED lamp was used as a light source to illuminate the combustor internal section.

A phantom high speed camera was used to capture the spherically expanding flame at a speed of 2000 frame per second. The recorded cine videos were then converted to image files for further analysis using image processing software. Adobe Photoshop image editing software was used to convert to the images of the spherical flames to binary images. These binary images were then analyzed using a Matlab script file to obtain flame area and later the radius. The obtained flame radii were then tabulated in a spreadsheet file and the flame speed was calculated by differentiating the flame radius with time in a first order fit of five points.

3. RESULTS AND DISCUSSION

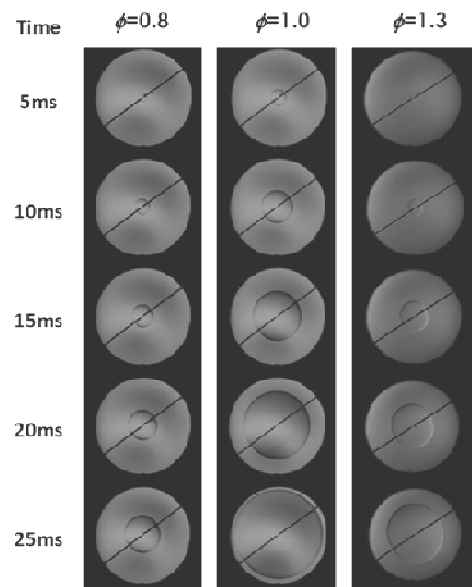


Figure 2. Development of spherical flame propagation of methane-air with central ignition.

Figure 2 shows development of methane-air spherical flame at different equivalence ratio of 0.8, 1.0 and 1.3. The circular boundary represents the size of the optical access windows and the black line crossing in each images is a pair of steel spark electrodes connected to the ignition system to initiate spark from central region. In general, throughout the propagation, all flames developed in a smooth spherical flame. The flame of stoichiometric equivalence ratio developed at a much faster rate compared to the flame at the equivalence ratio of 0.8 and 1.3. This corresponds to the characteristics of combustion where the flame speed tend to be higher at equivalence ratio

slightly than stoichiometric and lower in the rich or lean side[12].

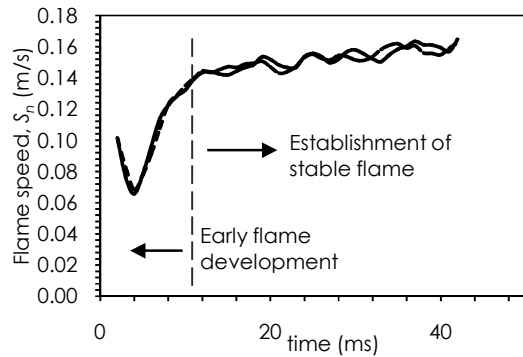


Figure 3. Variation of flame speed of methane-air mixture with time at equivalence ratio of 0.8

Figure 3 shows the variation of flame speed as a function of time at equivalence ratio of 0.8 from two identical experiments. The plot depicts a typical flame speed progress over time with a sharp decrease from the point of ignition to a certain time where it reaches a minimum pivotal point. This could be attributed to the radicals from the spark that rapidly dissipates until it reaches the minimum point [6]. The spark also creates shockwave that propagates outward, followed by a slower thermal wave. The thermal wave front usually has high initial speed that rapidly decreases over a short period of time [13]. From the minimum point, flame speed start to increase again until it stabilizes with time as the combustion progresses. Within this region normal chemistry predominate combustion as the radicals from the spark diminishes. Flame establishment can be estimated by the linear relation of flame speed against stretch rate which will be discussed later.

Both experiment shows similar trend with a slight variation suggesting good data reproducibility. The percentage of flame speed fluctuation after 15 ms onwards is around 6.3% which is considerably low. The noticeable fluctuation at 19 ms onwards could be linked to acoustic disturbances as observed by Gillespie et al [10]. The flame-acoustic disturbances is caused by an interaction between heat release and acoustic waves [14]. Curved flames (including spherical flame) are more susceptible to acoustic disturbances, where the propagating flame front is stretched and curved by acoustic waves [15]. This disturbance could also be influenced by combustor geometry [16].

Figure 4 shows the comparison of flame speed obtained from different equivalence ratio with respect to time. The trend of the flame speed development displays similar trend with a sudden decrease to a minimum point before it increase again to reach an approximately stable speed with noticeable fluctuation. It is interesting to note that, fluctuation commenced after around 15 ms for each experiment. The percentages of fluctuation are about 12%, 18% and 19 % for stoichiometric, 1.2 and 1.3 experiments, respectively. Apparently, fluctuation is more pronounced at higher equivalence ratio. This might suggest acoustic disturbance, as discussed earlier, is more prevalent at richer side.

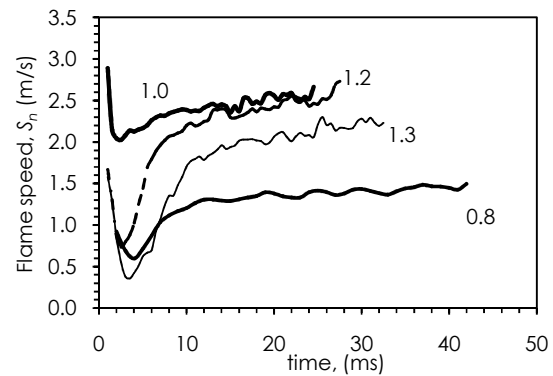


Figure 4. Variation of flame speed of methane-air mixture with time at equivalence ratio of 0.8, 1.0, 1.2 and 1.3.

In terms of trend, the initial flame speed and the point at which the minimum flame speed occurs is different from each condition. This point is highest for flame under stoichiometric condition followed by the flame of 1.2, 0.8 and 1.3. In the early stage of flame propagation, the flame is overcoming the quenching tendency due to high stretch rate arising from curvature effect[17]. Also, the flame speed of 0.8 progressed slower compared other experiments. This is followed by 1.3, 1.2 and lastly 1.0. This indicates the relative speed of the flame under different equivalence ratio. Flames that are either on the leaner or the richer side usually propagates slower than flame under stoichiometric condition. This is due to the disparity in thermal and mass diffusivity magnitude that would affect mass and heat transfer hence the flame propagation; whereas under stoichiometric condition, the magnitude of both thermal and mass diffusivity are equal[18]. The graph also reveals the time at which the flame stabilizes after ignition. The flames of each run

took approximately 10 ms to reach an approximately stable flame propagation.

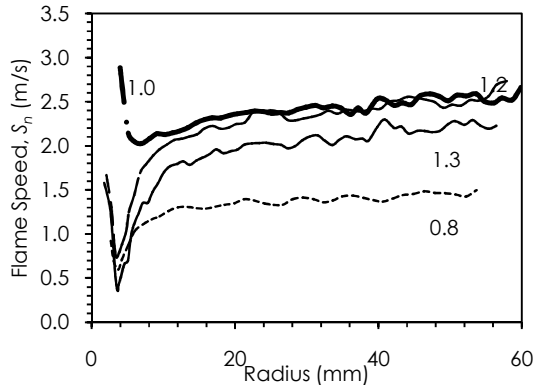


Figure 5. Variation of flame speed of methane-air mixture with radius at equivalence ratio of 0.8, 1.0, 1.2 and 1.3.

Figure 5 shows the plot of flame speed versus radius of methane-air mixture for experiments of 0.8, 1.2 and 1.3 equivalence ratios. The plot shows a periodically scattered data with a trend similar to flame speed variation with time. Fluctuation however is less pronounced in each experiment. At approximately 2 mm radius, the flame reaches its minimum value after ignition. The radius is about 1 mm larger for stoichiometric experiment. From this minimum point onwards, the flame development is due to normal chemistry. Data with radii less than 10mm should be discarded for burning rate calculation, as within this range the flame is significantly influenced by the radicals and shockwave from the spark [17].

Figure 6 shows the variation of methane-air mixture flame speed with stretch. The flame stretch here is defined as the time derivative of the spherical flame area of an infinitesimal element divided by the spherical flame area [10]. With the exception of stoichiometric experiment, the variation of flame speed for three other experiments i.e. for equivalence ratio of 0.8, 1.2 and 1.3 shares some similarities especially the characteristics twist during the early stage of flame propagation. This could be attributed to the effect of ignition energy and also to different stretch rate at the early stage of combustion at earlier stage of flame development [17]. Apparently stretch rate becomes more apparent under lean and rich region. Extrapolating flame speed to a point of zero stretch rate in Figure 6 yields unstretched flame speed, S_u while the slope

gives the Markstein length L_b . However, prior to extrapolation, some data especially those represent the early stage of combustion should be excluded as these data are generally affected by ignition spark and could lead to over or underestimation of unstretched flame speed.

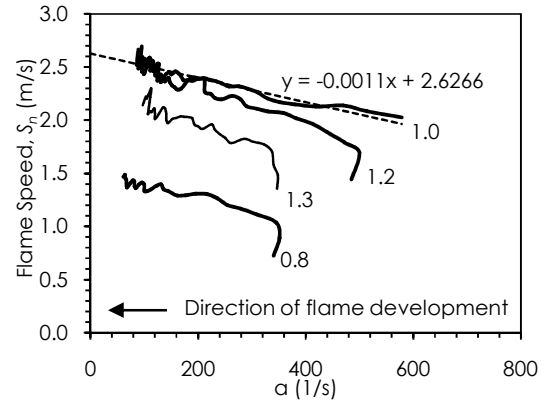


Figure 6. Variation of flame speed of methane-air mixture with stretch rate at equivalence ratio of 0.8, 1.0, 1.2 and 1.3.

The magnitude and signs of Markstein length indicates the effect of stretch on flame propagation. Positive Markstein length indicates that stretched flame speed decreases as stretch rate increases and the flame tend to restrain any disturbance at the flame front leading to flame stability [17]. In this case, the surface convex to the unburned area will be stretched in the opposite direction, and this will suppress flame speed, and the flame stabilizes. On the contrary, negative Markstein length indicates that flame speed increases proportionally with stretch rate, and flame surface will stretch in the same direction, inducing flame front instability in the process. Obviously from Figure 6, Markstein length for each equivalence ratio is positive with different magnitude as indicated by their relative slope. This value is consistent with the smooth flame observation as shown in Fig. 2 for all equivalence ratios.

Figure 7 shows comparison of laminar burning rates of methane-air mixture at different equivalence ratio between previous studies and current study. The laminar burning rates is calculated by multiplying the unstretched flame speed obtained from Fig. 6 with the density ratio of burned and unburned gas which computed under the assumption of adiabatic constant pressure combustion [6]. All plots were obtained by drawing a best fit curve through the data

points. The burning rate variation with equivalence ratio shows a quadratic trend with a characteristics peak at equivalence ratio of 1.1. The maximum of burning rates at slightly rich equivalence ratio was probably due to the combined effect of the adiabatic flame temperature and dissociation of combustion products.

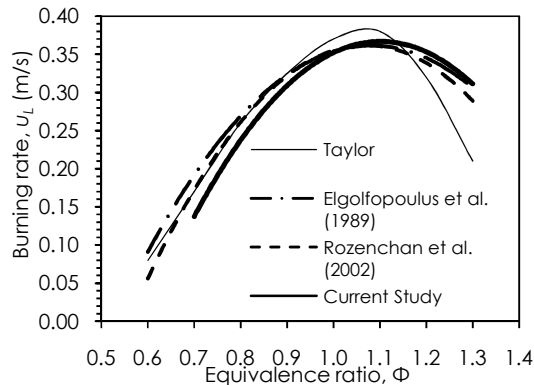


Figure 7. Comparison of methane-air mixture burning rate between present and previous works at equivalence ratio from 0.7 to 1.3.

It is shown that at equivalence ratio of 1.3, the burning rate is higher in this study at 0.31 m/s compared to observations by Rozenchan et al [7] and Elgolfopoulos et al [20] at 0.28 m/s, while Taylor [5] recorded the slowest burning rate at 0.21 m/s. This could be linked to the slightly higher initial temperature for this experiment at 302K. Marginal increase in unburned gas temperature may consequently increase the burning velocity [21]. Different methodology and the quality of data obtained from each study could also lead to different results [9]. This could be observed by results from [21] who used the counterflow methodology to determine the burning rate of methane-air mixture while both [5,7] used recorded schlieren images of spherically expanding flame.

4. CONCLUSION

In the present work, the combustion of methane has been studied by analyzing the spherical propagation flame of methane-air mixture in term of flame development, flame speed and the burning rates. Smooth and stable spherical flames were observed throughout flame development for all equivalence ratio. However, a small fluctuation of the flame speed after the spark influence region suggesting the presence of

acoustic disturbance in the later stage of flame propagation. This fluctuation varies from 7% and up to 19% as equivalence ratio was increased from 0.7 to 1.3, suggesting the influence of equivalence ratio on acoustic disturbance.

The burning rates of methane-air in this study shows a good agreement in comparison with the previous works. Apart from the experimental methodology, the quality of images obtained, image processing and the methods of data analysis could be considered as the source of uncertainties. The largest variation in terms of burning rate could be observed in the case of experiment with equivalence ratio of 1.3. This could be explained by the difference in initial temperature of this particular experiment which is slightly higher at 302K.

ACKNOWLEDGMENT

The authors would like to thank Ministry of Higher Education and Universiti Teknologi Malaysia for supporting this research activity under a Research Grant Scheme No. Q.J130000.2524.07H55.

REFERENCES

- [1] Bosschaart, K. J., de Goey, L. P. H. 2004. The laminar burning velocity of flames propagating in mixtures of hydrocarbons and air measured with the heat flux method. *Combust. Flame.* 136: 261–269.
- [2] Konnov, A. A., Dyakov, I. V., De Ruyck, J. 2003. Measurement of adiabatic burning velocity in ethane–oxygen–nitrogen and in ethane–oxygen–argon mixtures. *Exp. Therm. Fluid Sci.* 27: 379–384.
- [3] Chao, B.H., Egolfopoulos, F.N., Law, C.K. 1997. Structure and propagation of premixed flame in nozzle-generated counterflow, *Combust. Flame.* 109: 620–638.
- [4] Jackson, G.S., Sai, R., Plaia, J.M., Boggs, C.M., Kiger, K.T. 2003. Influence of H₂ on the response of lean premixed CH₄ flames to high strained flows. *Combust. Flame.* 132: 503–511.
- [5] Taylor, S. C. 1991. Burning velocity and the effect of flame stretch. PhD Thesis. University of Leeds.
- [6] Gu, X.J., Haq, M.Z., Lawes, M., Woolley, R. 2000. Laminar burning velocity and Markstein lengths of methane–air mixtures. *Combust. Flame.* 121: 41–58.
- [7] Rozenchan, G., Zhu, D. L., Law, C. K., Tse, S. D. 2002. Outward propagation, burning velocities, and chemical effects of methane flames up to 60 atm. *Proceedings of the Combustion Institute.* 29: 1461–1469.

- [8] Hassan, M.I., Aung, K. T., Faeth, G. M. 1998. Measured and predicted properties of laminar premixed methane/air flames at various pressures. *Combust. Flame*. 115: 539–550.
- [9] Tahtouh, T., Halter, F., Mounaim-Rousselle, C. 2009. Measurement of laminar burning speeds and Markstein lengths using a novel methodology. *Combustion and Flame*. 156: 1735–1743.
- [10] Gillespie, L., Lawes, M., Sheppard, C. G. W., and Woolley, R. 2000. *Aspects of Laminar and Turbulent Burning Velocity Relevant to SI Engines*. Society of Automotive Engineers.
- [11] Hinton, N., Stone, R. 2014. Laminar burning velocity measurements of methane and carbon dioxide mixtures (biogas) over wide ranging temperatures and pressures. *Fuel* 116: 743-750.
- [12] Turns, S. R. 2012. *An Introduction to Combustion: Concepts and Applications*. 3rd edition. New York: McGraw Hill.
- [13] Bradley, D., Lung, K. K. 1987. *Combust. Flame*. 69:71.
- [14] Zhang, Z., Guan, D., Zheng, Y., and Li, G. 2015. Characterizing premixed laminar flame-acoustics nonlinear interaction. *Energy Conversion and Management*. 98: 331–339.
- [15] Shalaby, H., Luo, K. H., Thévenin, D. 2014. Response of curved premixed flames to single-frequency and wideband acoustic waves. *Combustion and Flame*. 161: 2868–2877.
- [16] Movileanu, C., Gosa, V., Razus, D. 2015. Propagation of ethylene-air flames in closed cylindrical vessels with asymmetrical ignition. *Process Safety and Environmental Protection*. 96: 167–176.
- [17] Bradley, D., Gaskell, P., Gu, X. 1996. Burning velocities, Markstein lengths, and flame quenching for spherical methane-air flames: a computational study. *Combust Flame*. 104(1–2):176–98.
- [18] Poinot, T., Veynante, D. 2005. *Theoretical and Numerical Combustion*. 2nd edition. Philadelphia: R.T. Edwards.
- [19] Miao, H., Liu, Y. 2014. Measuring the laminar burning velocity and Markstein length of premixed methane/nitrogen/air mixtures with the consideration of nonlinear stretch effects. *Fuel*. 121: 208–215.
- [20] Elgolfopoulos, F. N., Cho, P., and Law, C. K. 1989. Laminar flame speeds of methane-air mixtures under reduced and elevated pressures. *Combustion and Flame*. 76 (3-4); 375-391.
- [21] Bradley, D., Hundy, G. F. 1971. Burning velocities of methane-air mixtures using hot-wire anemometers in closed-vessel explosions. *Symposium (International) on Combustion*. 13 (1): 575-583.